detector tracks the focal spot center. Defocus is positive when the detector goes farther from the mirror. The effect of a yaw misalignment is a broadening of the focal spot in the shape of an arc, along with a rotation in the detector plane (Figure 10) i.e., non-parallel to the mirror surface. Were θ and z already aligned, we could simply act the related motor until the image size gets minimized. This will rarely be the case, but also in the presence of other misalignments, one can always optimize δ by having the arc lie upright in the image and minimized in size (Figure 11). We can then assume that δ can be corrected to within ± 8 arcsec. In all these images, the detector is oriented like an observer looking at the X-ray source (i.e., Pantolski is at left).

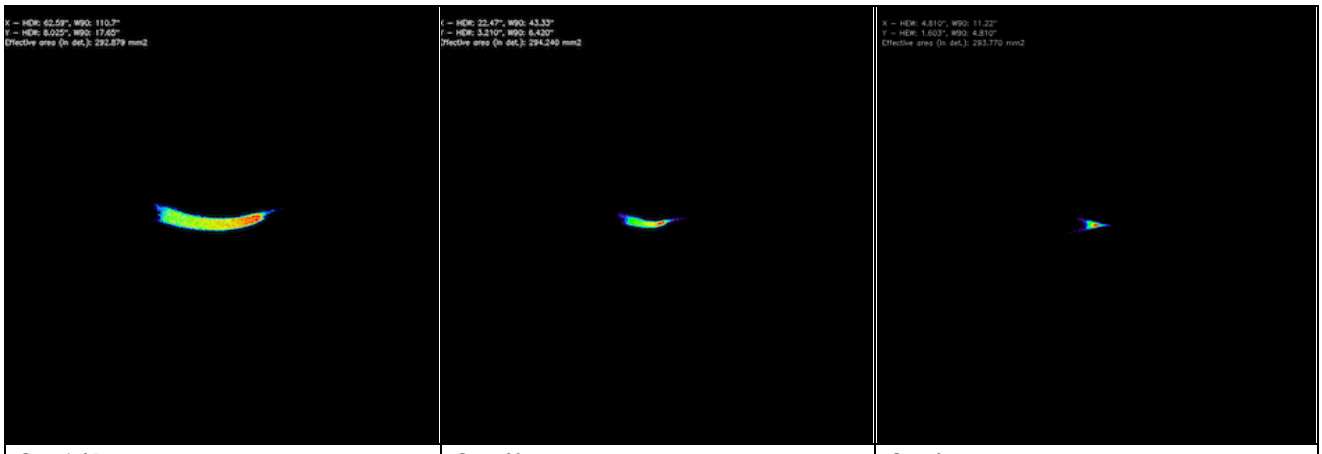

δ = 165 arcsec	δ = 60 arcsec	δ = 0 arcsec

Figure 10: simulated alignment of the yaw angle δ, by nulling off-axis aberration if the pitch angle and the focal distance are correctly aligned, with the diverging beam. The detector size is ½ of PIXI (and so is in Figure 11).

δ = 165 arcsec	δ = 33 arcsec	δ = 0 arcsec

Figure 11: simulated alignment of the yaw angle δ, if the pitch angle and the focal distance are NOT aligned off-axis, with the diverging beam at 1.49 keV. This time, a pitch misalignment θ = +83 arcsec was added.

The alignment in θ (the pitch angle, Figure 12) can be more complex, because it is linearly correlated to the mirror de-focus (Figure 13): *decreasing the incidence angle by 1 arcmin increases the focal length by approx. 94 mm* (and vice versa, see Figure 14, left). Nevertheless, the HEW reaches its global minimum only when both the incidence angle and the detector distance equal the nominal ones. In order to find the mirror alignment, the best focus search should in principle be repeated changing the pitch angle and taking the minimum HEW for each z-scan. Then, plotting the values of the minima as a function of θ (Figure 14, right) and locating the minimum will allow us to determine the correct alignment and focal length (in order to keep the focus centered in the detector, each movement Δz along the optical axis also entails a lateral displacement of the beam $\Delta z \tan 2\alpha \approx 0.0318\, \Delta z$). This method, however, can be somehow impractical.

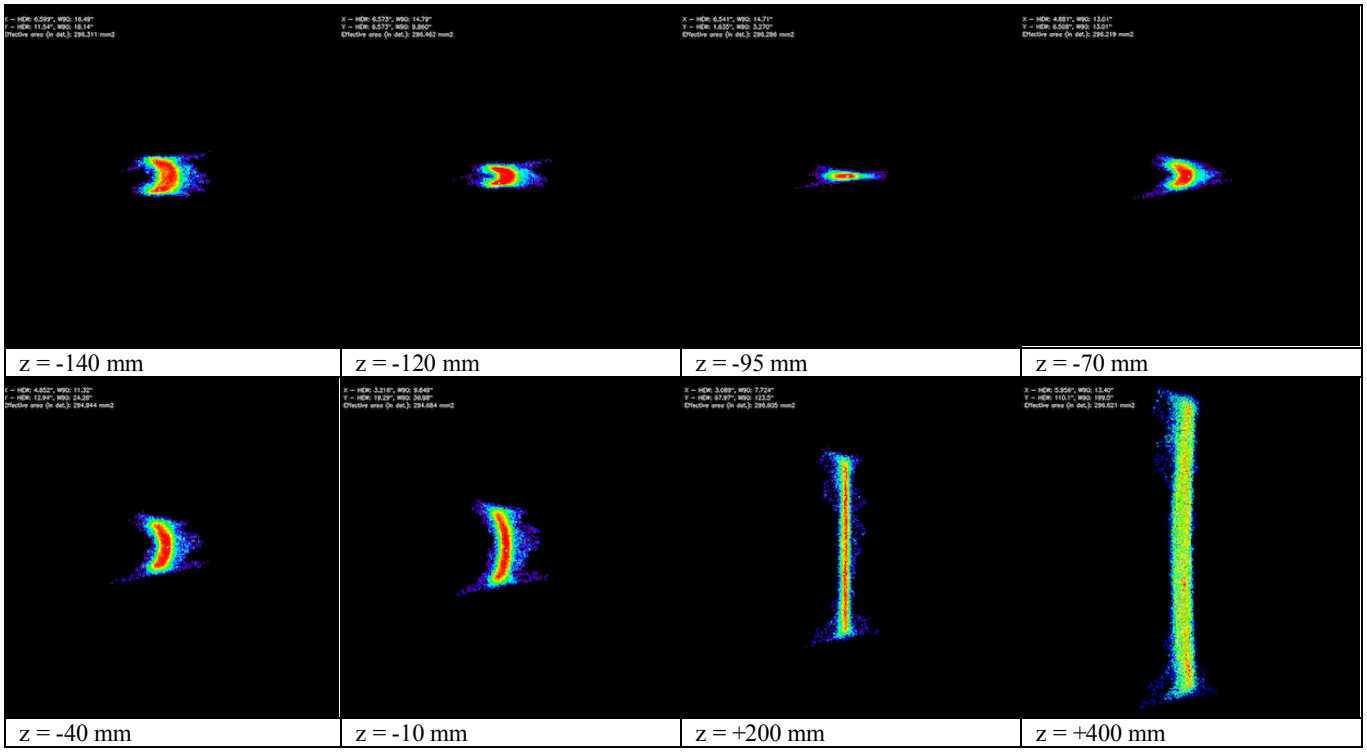

Figure 12: simulated focus search scan with the parabola misaligned in pitch angle by θ = +1 arcmin, with the diverging beam at 1.49 keV; the smallest spot does not occur at the correct focal length. The yaw angle is correctly aligned. The detector size is 5 mm.

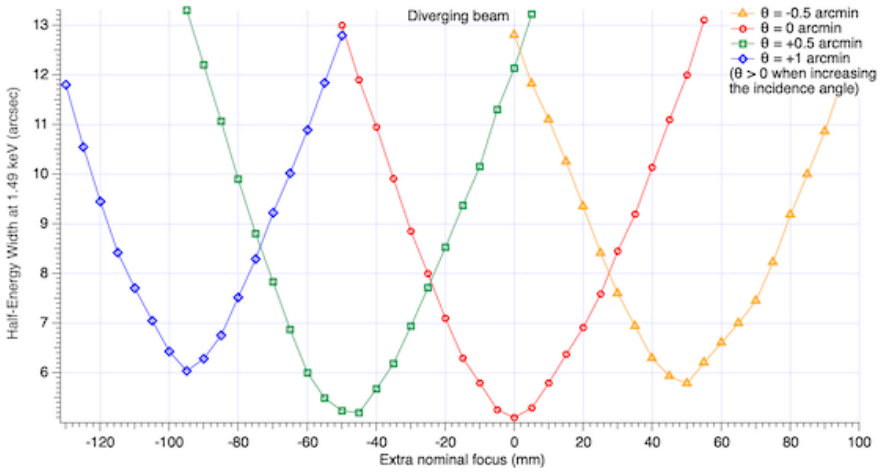

Figure 13: focus search ad different horizontal alignments, under diverging beam illumination.

Due to the slow variation of the HEW with the pitch angle at the best focus, it seems unlikely to determine the pitch angle to accuracy better than 0.5 arcmin and consequently, to determine the focal length to better accuracy than a few centimeters. Looking at the shape of the focal spots in Figure 12 and Figure 15, we can notice a peculiarity of the alignment under diverging beam: the arc remains concave on the left side (i.e. toward Pantolski), passing from one side to the other of the best focus, in both θ-scans and z-scans. Concavity inversion occurs for large deviations of the pitch angle or the detector distance; therefore, the arc concavity cannot be used to determine whether the detector is either intra- or extra-focal. This would not occur, however, under parallel beam illumination (Figure 20).

A friendly suggestion of an alignment process is shown, step by step, in Figure 16. Basically, once an "acceptably small" focal spot is found, every step in the true focus search consists of a pitch rotation and a focus correction in the ratio $\Delta\theta$ = -1 arcmin $\leftrightarrow$ Δz = +94 mm. In out of focus position, concavity always faces the Pantolski side.

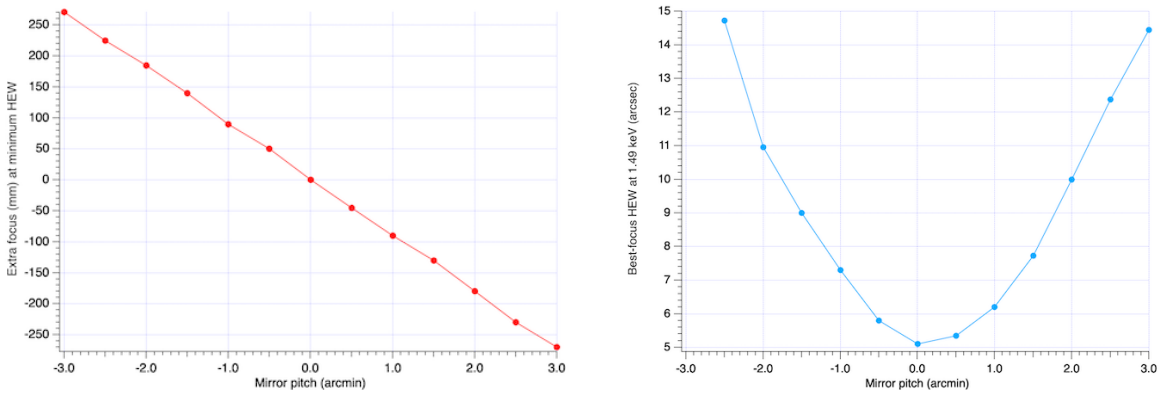

Figure 14: (left) variation of the best focal distance with θ, under diverging beam illumination. The trend is linear within the uncertainty of a few millimeters. (right) HEW variation in the best focus for different values of θ.

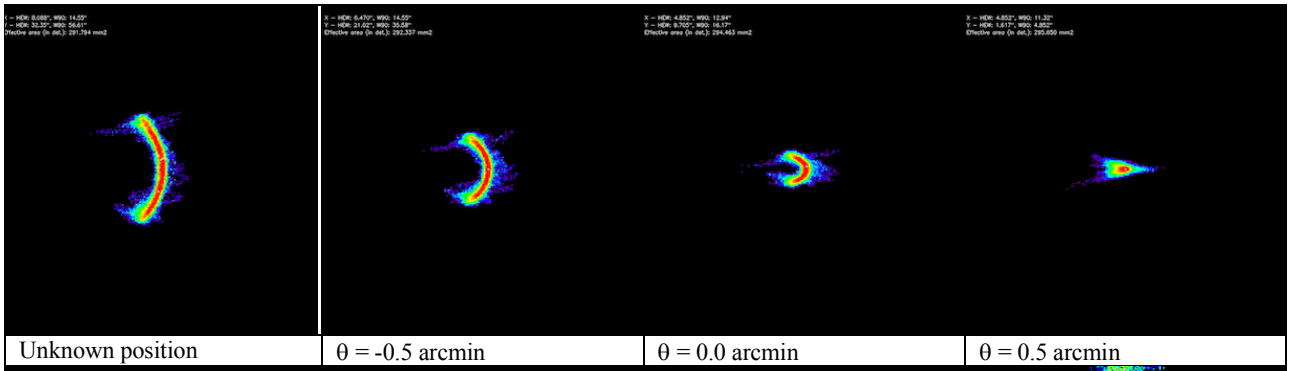

Figure 15: simulated scan of the pitch angle θ, assuming that the yaw angle was corrected as in Figure 11, with the diverging beam at 1.49 keV. The focal plane is kept fixed intra-focus by 4 cm, therefore the smallest spot does not occur at θ = 0 arcmin. The detector size is 5 mm.

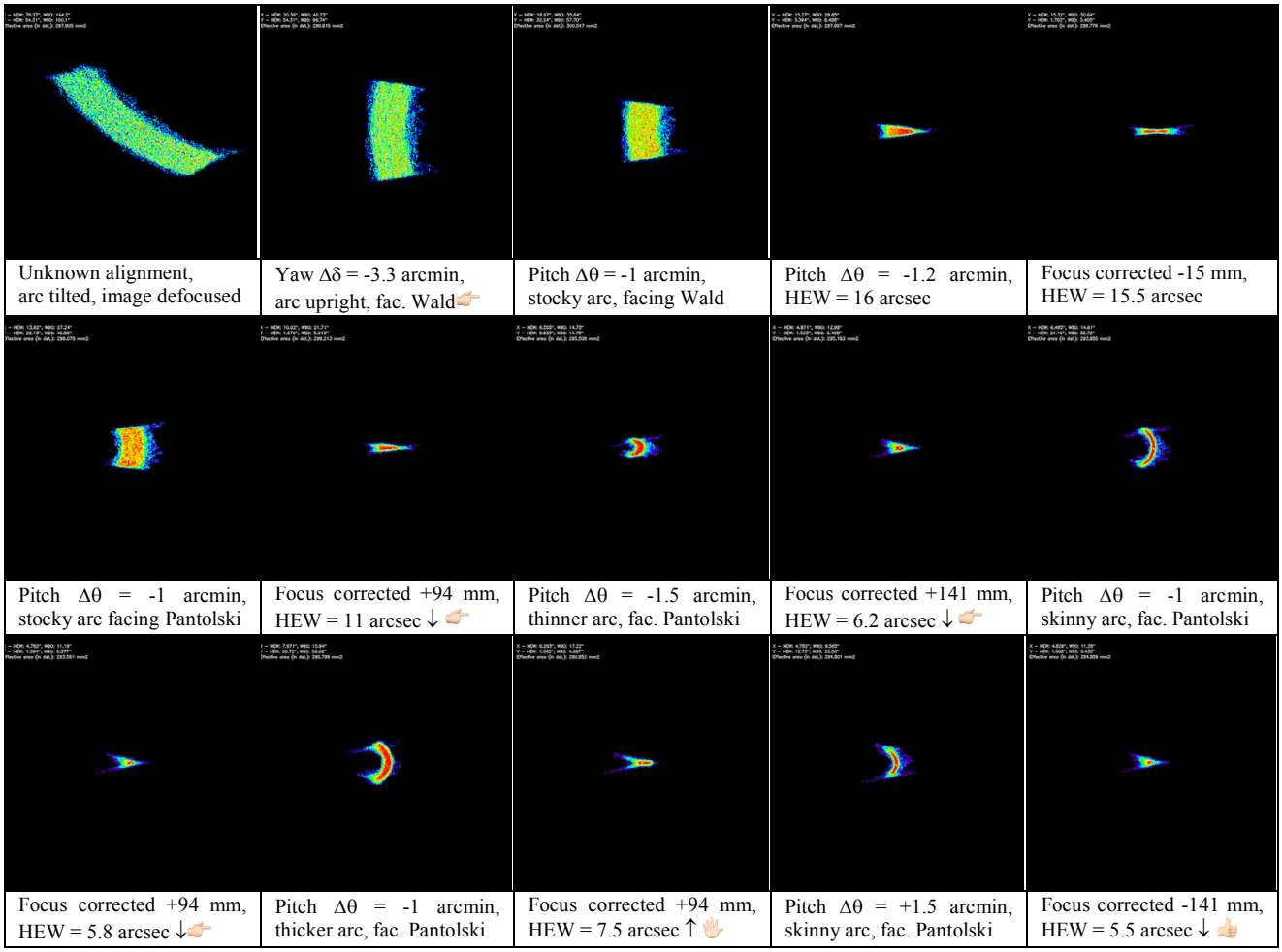

Figure 16: a simulated alignment process with the diverging beam *at 1.49 keV. The detector size is ¼ of PIXI's.*

3.1.3. *Measurement in the best focus*

Once the best focus is found under diverging beam, the measurement at 1.49 keV as modelled from the profile and the surface metrology is shown in Figure 17, with a predicted HEW = 5.2 arcsec. The triangular shape is related to the setup with the source at finite distance (Figure 9, center). We list in Table 1 and Table 2 the calculated effective area and angular resolution values.

Table 1: effective area values of the BEaTriX mirror, before coating at DTU. The area refers to an illumination of the central 400 mm 60 mm area. The effective area is essentially unaffected by the low divergence of the beam.

	Without coating	
	Parallel beam	*Diverging beam*
Geometric area	365 mm^2	364 mm^2
Effective area at 1.49 keV	295 mm^2	293 mm^2
Effective area at 4.51 keV	< 1 mm^2	< 1 mm^2

Table 2: expected angular resolution of the uncoated BEaTriX mirror with the PANTER source, seen by PIXI.

	1.49 keV
Perfect mirror, diverging beam	4.8 arcsec
Perfect mirror, parallel beam	1.6 arcsec
Real mirror, diverging beam	5.2 arcsec
Real mirror, parallel beam	3.3 arcsec

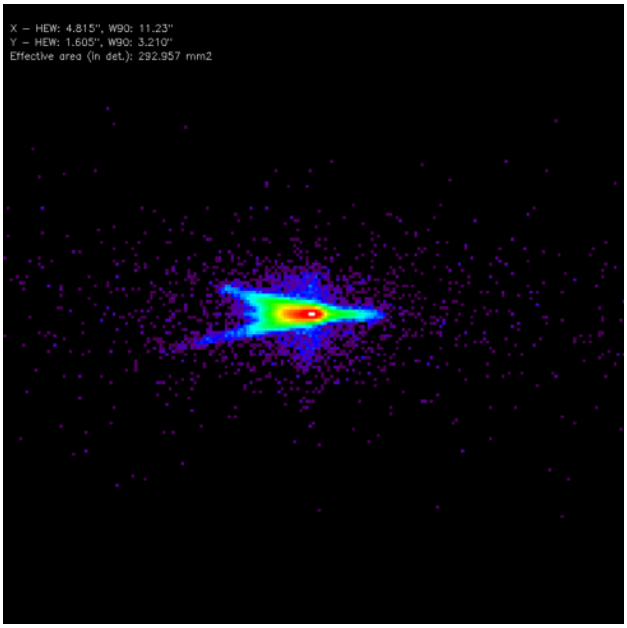

Figure 17: ray-tracing result from the actual metrology of the uncoated mirror *at 1.49 keV (Sect. 2.2), in the best focus with* diverging beam *and PIXI (**HEW = 5.2 arcsec**). The frame size is 4 mm, log colorscale.*

3.1.4. Measurement in intra-focus position

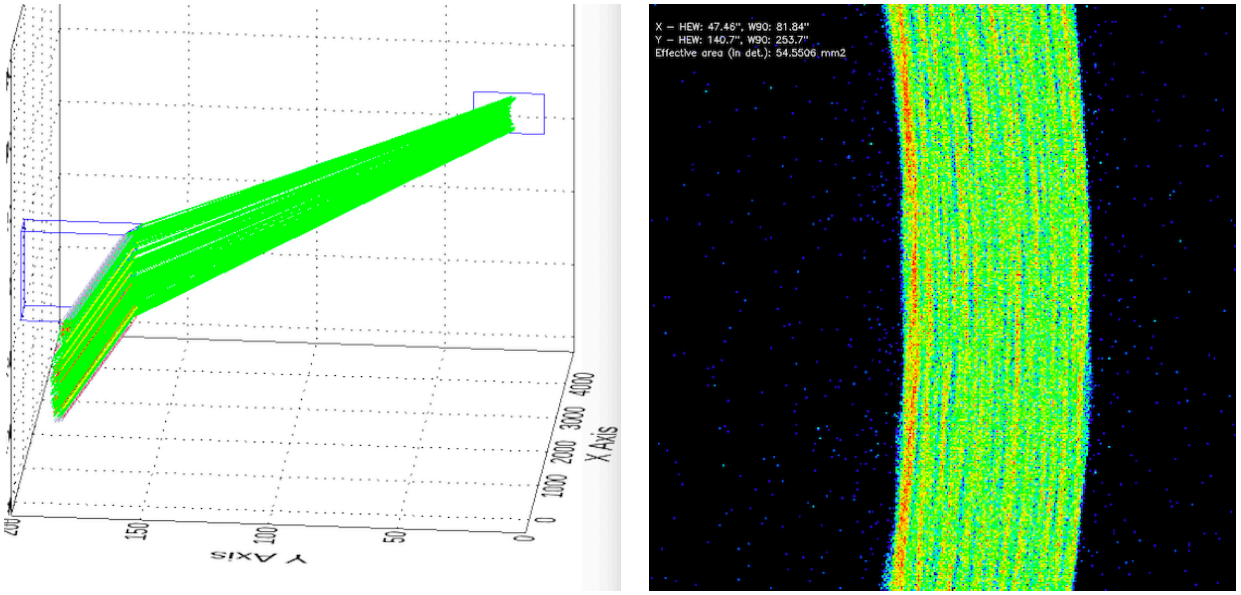

Figure 18: (left) ray-tracing result from the actual metrology, in intra-focal setup (z = -100 mm, θ = -20 arcmin). The intra-focal arc is entirely within the PIXI area. (right) zoomed view on the central 5 mm × 5 mm.

After mirror and detector alignment in focus, and the exposure in the best focus, it can be interesting to obtain an intra-focal image that provides useful insights on the mirror shape [RD10]. As the stage carrying the detector cannot exceed a ± 200 mm displacement along the beam, effective defocusing can be obtained changing the pitch angle by -20 arcmin (i.e., reducing the incidence angle by 20 arcmin) and approaching the detector by 100 mm. In this way, the de-focused image can be captured within the PIXI area. At the same time, the image magnification is sufficient to resolve the typical striations, chiefly caused by the longitudinal errors. In Figure 18, we show a zoomed view of the intra-focus arc.

3.2. Alignment and measurement in parallel beam at 1.49 keV

Once the mirror is aligned in the diverging beam, the ZP can be inserted into the beam to make it parallel. If the source did not move after insertion of the ZP, the mirror can be simply refocused approaching the detector to the mirror by 200 mm.

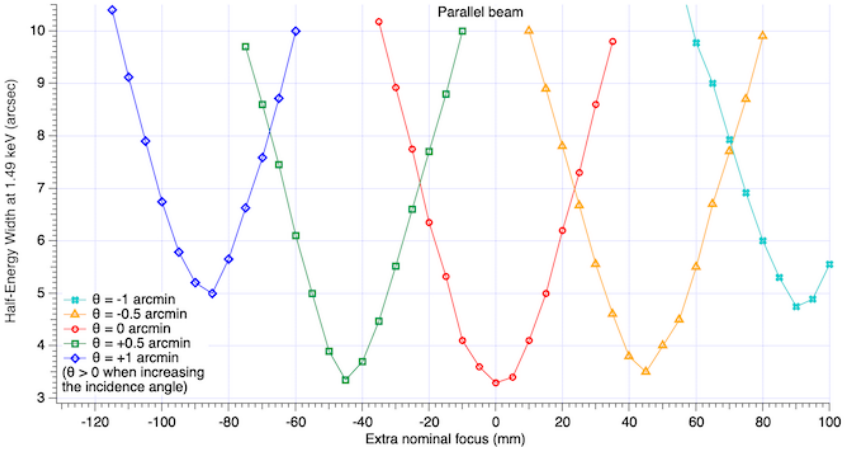

Figure 19: focus search curves at different pitch angles, under parallel beam *illumination. They resemble the ones seen in Figure 16, only narrower and sharper.*

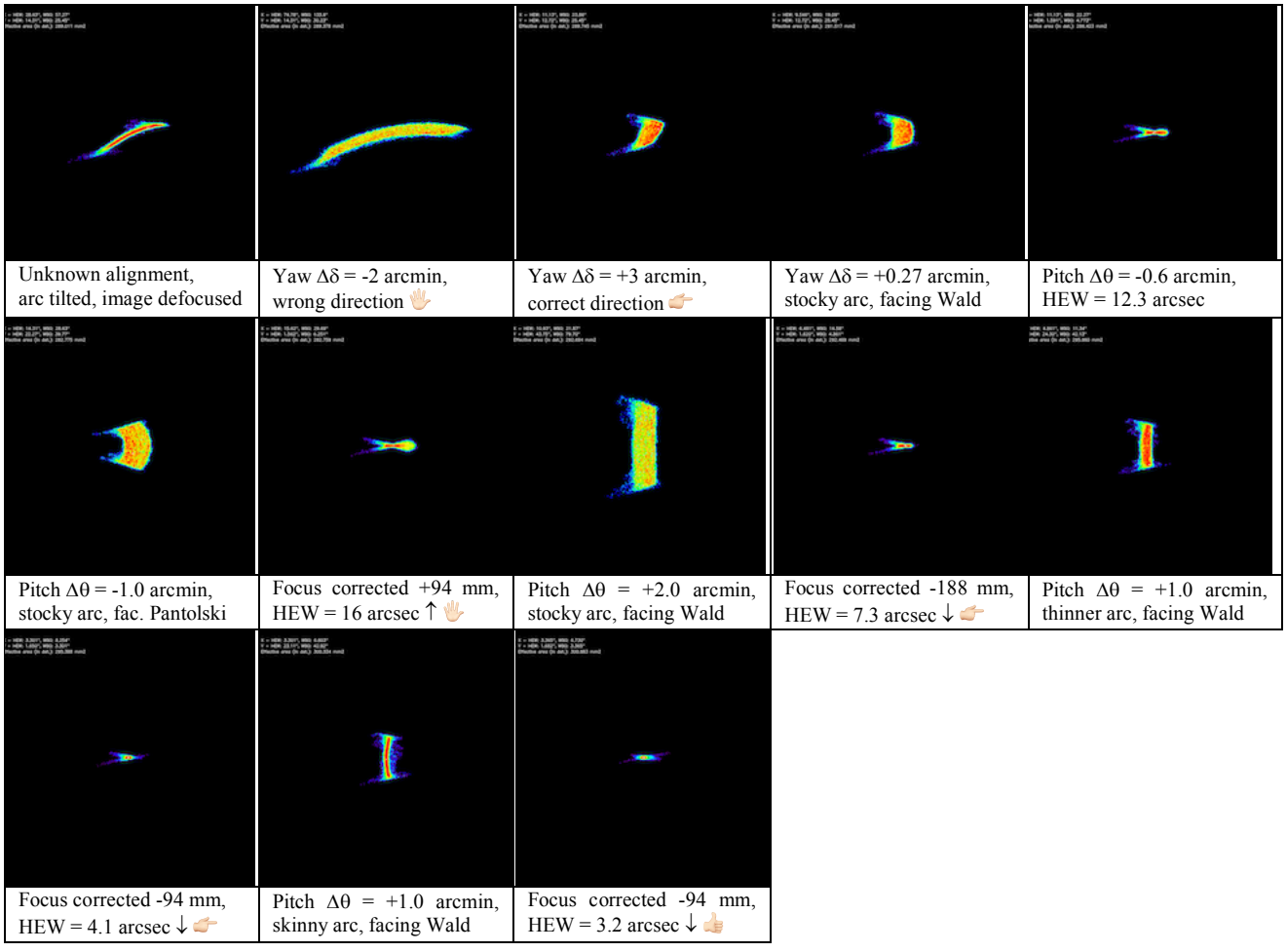

Figure 20: simulated alignment process with the parallel beam *at 1.49 keV. The detector size is ¼ of PIXI's.*

If needed, the mirror focusing can be refined: the focal distance depends on the incidence angle, just like the case of the diverging beam. Just like the previous case, the best focus markedly depends on θ, and the smallest focal spot is reached only when the alignment and focal distance are correct, even to within an uncertainty of a 3-4 cm in focus and of 0.5 arcmin in the pitch angle (Figure 19). In parallel beam setup, the change in focus due to pitch angle variations is nearly the same as the one found with the diverging beam: $\Delta\theta$ = -1 arcmin $\rightarrow$ Δz = +94 mm. In contrast, this time the arc changes concavity (towards Pantolski $\leftrightarrow$ Wald) passing by the smallest focus in a z-scan or a θ-scan. Should it be needed, we report in Figure 20 a suggestion for mirror alignment with the parallel beam.

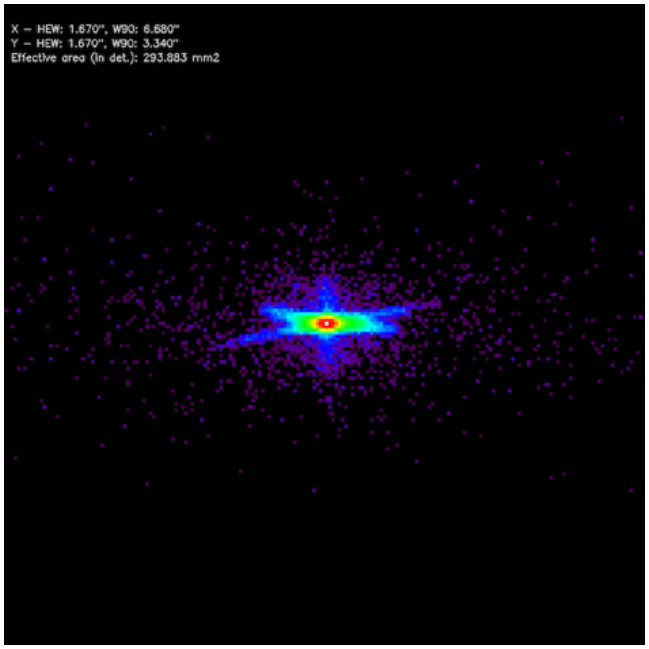

Figure 21: ray-tracing result from the actual metrology of the uncoated mirror *at 1.49 keV (Sect. 2.2), in the best focus with the ZP and PIXI (**HEW = 3.3 arcsec**). The frame size is 4 mm, log colorscale.*

The image in focus will expectedly look like the one shown in Figure 21. The image will resemble Figure 6, only degraded by the angular dimensions of the X-ray source. We expect to measure a HEW value of **3.3 arcsec**.

4. Test plan at PANTER, after coating

After the deposition of the platinum coating at DTU, the mirror will return to PANTER to repeat all the alignment and test sequence described in the previous sections. A measurement *at 4.51 keV is also needed,* because this is the energy of operation for this BEaTriX mirror. As the ZP will not work at 4.51 keV, the test at this energy can only be performed in diverging setup. The impact of the scattering should be only slightly larger at higher energy (a few tenths of arcsec). We recapitulate in Table 3 the expected effective area values with and without coating, and the expected HEW values in the two cases. The simulations of the focal spots at the two energies in the two settings are displayed in Figure 22 and Figure 23.

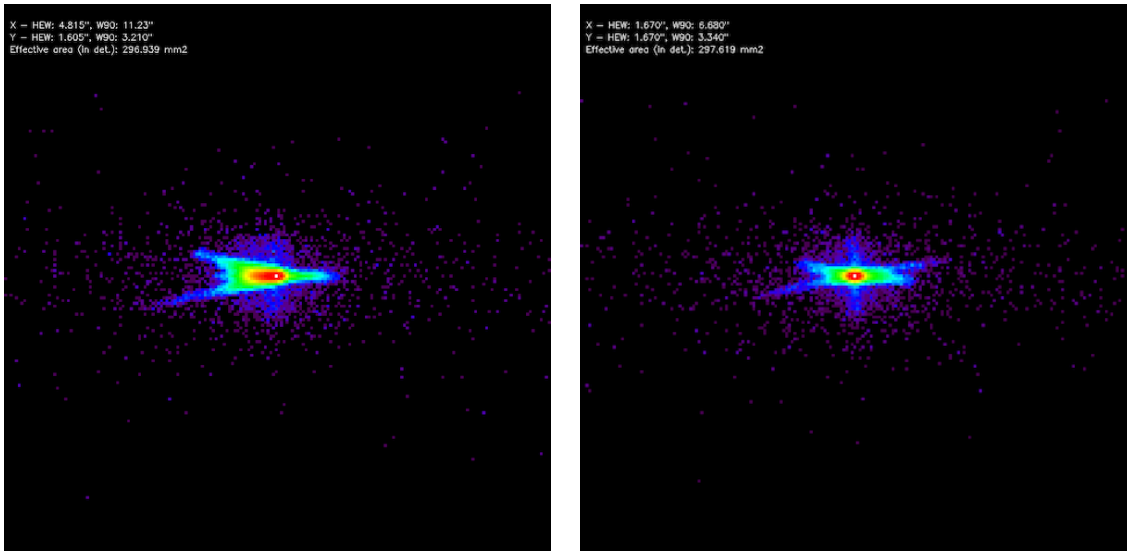

*Figure 22: ray-tracing result from the actual metrology of the coated mirror at 1.49 keV (Sect. 2.2), in the best focus with (left) a diverging beam and PIXI, (right) with the ZP and PIXI. The frame size is 4 mm, log colorscale. HEW values are **5.2 arcsec** and **3.3 arcsec**.*

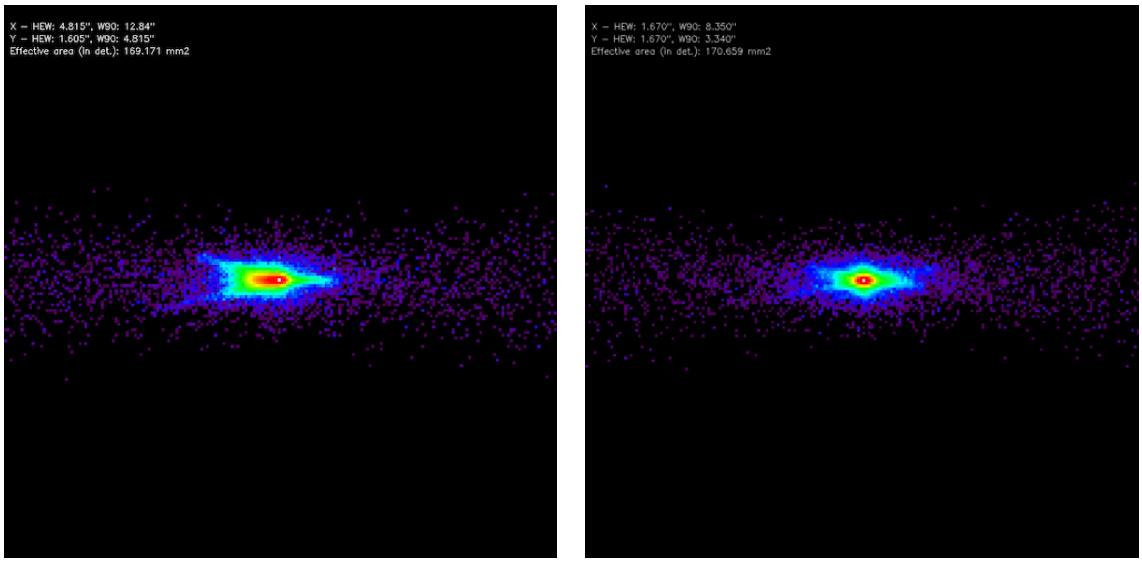

*Figure 23: ray-tracing result from the actual metrology of the coated mirror at 4.51 keV (Sect. 2.2), in the best focus with (left) a diverging beam and PIXI, and (right, theoretically) with a parallel beam and PIXI. The frame size is 4 mm, log colorscale. HEW values are **5.4 arcsec** and **3.5 arcsec**.*

5. Conclusions

In this document, we have reported a description of the expected results of the PANTER tests, and briefly discussed the test setup. We have suggested a possible alignment procedure. For convenience, some numerical results are listed in the tables below.

Table 3: effective area values of the BEaTriX mirror after coating at DTU. The area refers to an illumination of the central 400 mm 60 mm area. The effective area is unaffected by the low divergence of the beam.

	With Pt+Cr coating	
	Parallel beam	*Diverging beam*
Geometric area	365 mm^2	364 mm^2
Effective area at 1.49 keV	298 mm^2	298 mm^2
Effective area at 4.51 keV	172 mm^2	173 mm^2

Table 4: expected angular resolution of the coated BEaTriX mirror with the PANTER source, seen by PIXI.

	1.49 keV	***4.51 keV***
Perfect mirror, div. beam	4.8 arcsec	4.8 arcsec
Perfect mirror, par. beam	1.6 arcsec	1.6 arcsec
Real mirror, diverging beam	5.2 arcsec	5.4 arcsec
Real mirror, parallel beam	3.3 arcsec	3.5 arcsec